Received: 6 March 2024 | Revised: 23 May 2024 | Accepted: 27 May 2024

DOI: 10.1002/ajhb.24115

ORIGINAL ARTICLE

American Journal of Human Biology WILEY

# What's luck got to do with it? A generative model for examining the role of stochasticity in age-at-death, with implications for bioarchaeology

**Bronwyn Wyatt**[1] | **Amy Anderson**[2,3] | **Stacey Ward**[1] | **Laura A. B. Wilson**[1,4,5]

[1]School of Anthropology and Archaeology, The Australian National University, Acton, Australian Capital Territory, Australia

[2]Lise Meitner Research Group BirthRites, Max Planck Institute for Evolutionary Anthropology, Leipzig, Germany

[3]Department of Human Behavior, Ecology and Culture, Max Planck Institute for Evolutionary Anthropology, Leipzig, Germany

[4]School of Biological, Earth and Environmental Sciences, UNSW, Sydney, New South Wales, Australia

[5]ARC Training Centre for M3D Innovation, Research School of Physics, The Australian National University, Acton, Australian Capital Territory, Australia

**Correspondence**
Bronwyn Wyatt, School of Anthropology and Archaeology, The Australian National University, Acton, ACT 2601, Australia.
Email: bronwyn.wyatt@anu.edu.au

**Funding information**
Australian National University Research Scholarship, Grant/Award Number: 738/2018; Australian Government Research Training Program Scholarship; Australian Research Council, Grant/Award Number: FT200100822

## Abstract

**Introduction:** The role of "luck" in determining individual exposure to health insults is a critical component of the processes that shape age-at-death distributions in mortality samples but is difficult to address using traditional bioarchaeological analysis of skeletal materials. The present study introduces a computer simulation approach to modeling stochasticity's contribution to the mortality schedule of a simulated cohort.

**Methods:** The present study employs an agent-based model of 15,100 individuals across a 120 year period to examine the predictive value of birth frailty on age-at-death when varying the likelihood of exposure to health insults.

**Results:** Birth frailty, when accounting for varying exposure likelihood scenarios, was found to account for 18.7% of the observed variation in individual age-at-death. Analysis stratified by exposure likelihood demonstrated that birth frailty alone explains 10.2%–12.1% of the variation observed across exposure likelihood scenarios, with the stochasticity associated with exposure to health insults (i.e., severity of health insult) and mortality likelihood driving the majority of variation observed.

**Conclusions:** Stochasticity of stressor exposure and intrinsic stressor severity are underappreciated but powerful drivers of mortality in this simulation. This study demonstrates the potential value of simulation modeling for bioarchaeological research.

## 1 | INTRODUCTION

Understanding the health and well-being of past populations is a key concern for bioarchaeologists and is traditionally explored through the contextualized analysis of skeletal indicators of stress and disease. More recently, however, a more specific focus on the vulnerability or resilience of individuals to health insults ("frailty") has been favored in response to recognition of the complexity, and ambiguity, of defining "health" even in modern contexts (Reitsema & Mcilvaine, 2014; Temple & Goodman, 2014). What constitutes frailty differs depending on the specific research question, with both accumulation of morbidity as inferred by skeletal indicators (Marklein et al., 2016; Steckel et al., 2002; Zedda et al., 2021) and increased risk of mortality (DeWitte & Wood, 2008, Yaussy et al., 2023, Wissler & Dewitte, 2023) referred to as frailty or associated concepts (poor health, lowered resilience, etc.) in bioarchaeological contexts. The present study employs the latter meaning of individual frailty—that is, frailer individuals face greater likelihood of mortality and a subsequently reduced age-at-death in relation to their peers, as conceptualized by the work of Vaupel et al. (1979) and thus employs age-at-death as a means of measuring frailty.

This relational definition of frailty underpins the use of hazard analysis as a means of identifying frail individuals or, more accurately, the personal characteristics associated with greater mortality risks (Usher (2000), DeWitte and Wood (2008), and Yaussy et al. (2016)). Here, characteristics associated with greater frailty (a greater likelihood of mortality compared to others of the same age) is interpreted as indicators of greater stressor exposure and/or poor resilience to health insults.

The demographic literature, however, emphasizes that frailty is probabilistic, not deterministic that is, the differences in individual exposures to health insults, and the varying nature of those health insults, complicates the likelihood of mortality at both the individual and population levels, even in a theoretical birth cohort with uniform frailty (Caswell, 2014; Hartemink et al., 2017; Van Daalen & Caswell, 2020). In light of this consideration, even correlational relationships between a given skeletal indicator and mortality risk must also account for the stochastic nature of health insult exposure across the lifespan and across the study population. It is important here to note that this individual stochasticity is not the same as heterogeneity in mortality risk across a cohort due to individual frailty, but rather may be thought of as the "luck" (or lack thereof) component in avoiding or being exposed to a health insult and the nature of this specific insult if exposed (Caswell, 2009; Snyder & Ellner, 2018; Van Daalen & Caswell, 2020). In more concrete terms, it reflects individual, nonfixed heterogeneity that appears as chance, pending improved knowledge of causal drivers of insult exposure likelihood and effect (e.g., the prevalence and severity of a given viral strain).

Thus, there are two types of "hidden heterogeneity" in frailty. The first is conceived of as variation in the value of individual frailty among the members of a cohort. This is a stable individual trait present from birth, which encompasses all the ways in which individuals may differ with respect to mortality risk and is independent of other individual traits (Tuljapurkar et al., 2009). For clarity, this article will henceforth refer to this individual frailty at birth as heterogeneous frailty. The second type is the aforementioned individual stochastic frailty, hereafter referred to as stochastic frailty. Heterogeneous frailty therefore remains a constant proportional multiplier of an individual's age-specific mortality hazards throughout life. Stochastic frailty (or the likelihood and severity of insult exposure), by contrast, varies across the lifespan and appears to arise as a result of chance even when all other factors are equal.

Labeling of heterogeneous and stochastic frailty may seem little more than semantics—after all, they may both be broadly conceptualized as hidden heterogeneity in mortality risk—however, theoretical demographic modeling demonstrates the critical role that stochasticity ("luck") has on individual longevity (Caswell, 2009; Hartemink et al., 2017). Hartemink et al. (2017) report that "known" heterogeneity (here, birth frailty) accounted for less than 10% of cohort longevity variance in a cohort simulation, a result which challenges the view of fixed heterogeneity across the lifespan, a key assumption in the Gompertz or Gompertz–Makeham models of frailty which are frequently used to explore mortality risk in bioarchaeological research (Hartemink et al., 2017).

An additional factor to consider in modeling stochastic frailty is the role of recovery from a physiological insult. Although common in multistate models of health employed by epidemiologists and health researchers (Bijwaard, 2014), the adaption of such models to bioarchaeological data has generally treated transition to frailty as a unidirectional process owing to the use of skeletal indicators as a proxy of insult exposure, although Usher has also presented a four-state model which allows for recovery in the form of "healed" (nonactive) lesions (Dewitte & Wood, 2008; Usher, 2000). The focus of these models tends to be the exploration of enduring frailty into adulthood resulting from health insults in early life, which cause skeletal indicators of interest. Mortality hazard analysis is largely constrained to adults due to the complexity of accommodating developmental windows for skeletal indicators that form in childhood, when the presence or absence of these skeletal indicators is not yet

a fixed characteristic of all individuals in the sample (Dewitte & Hughes-Morey, 2012). However, incorporating the process of physiological recovery further increases the potential stochasticity at play, as recovery from an insult decreases an individual's accumulated frailty but is also constrained by the individual's capacity to recover.

Thus, there is a clear need to examine the interaction between individual heterogenic frailty and stochasticity of insult exposure, severity, and recovery. The contribution of potential causal drivers of a given age-at- death such as heterogenic frailty, however, remain difficult to disambiguate as it is not possible to run such experiments on populations of the past (or indeed, the present). An alternative option is to run experiments on simulated populations. Computer simulations enable flexible and repeatable experiments that can test causal drivers of complex population dynamics.

Agent-based modeling (ABM) is a specific method of computer simulation which can be used to develop and test hypotheses about complex systems that cannot be readily understood or for which group-level outcomes are emergent properties that cannot be predicted from knowledge of the individual components (Romanowska et al., 2021). An ABM is initiated by generating a set number of individuals (agents) with assigned characteristics (e.g., sex or health status). These agents are then placed in a simulated scenario based upon a set of rules to explore how they fare, and the results are analyzed for the influence of assigned characteristics on individual and group-level outcomes (Romanowska et al., 2021).

ABM has been widely adopted in the fields of demography, epidemiology, and ecology, as well as growing use in archeological modeling projects such as the exploration of the 1918 flu epidemic in central Canada (Carpenter & Sattenspiel, 2009; O'Neil & Sattenspiel, 2010), and population decline and collapse in the American Southwest (Axtell et al., 2002; Swedlund et al., 2016). The use of ABM in bioarchaeology specifically, however, is presently in its infancy despite the potential value it may hold in better understanding population dynamics of the past (see Galeta and Pankowská (2023)). The present study uses ABM to explore the influence of stochasticity on individual age-at-death (here a measurable representation of frailty), as well as to demonstrate the utility of such an approach for bioarchaeological research more broadly.

## 2 | METHODS

### 2.1 | Software

The ABMs described in this study were programmed using the R Statistical Software (R Core Team, 2021). The simulation model was programmed using Base R, with additional analysis using the following packages: "tidyverse" for tidying, and summarization of data (Wickham et al., 2019), "broom" for converting statistical objects for presentation (Robinson et al., 2023), "kableExtra" for presentation of results (Zhu, 2023), "ggplot2" for all figures (Wickham, 2016) with colors for figures generated using the "wesanderson" package (Ram & Wickham, 2018) and regression lines added using "ggpmisc" (Aphalo, 2023).

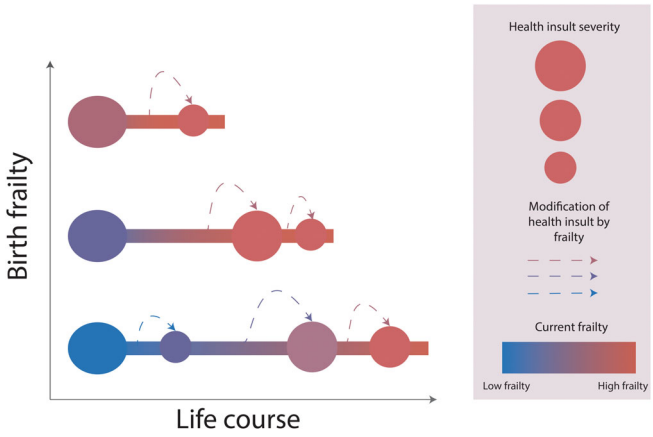


**FIGURE 1** Summary diagram of model components. Figure 1 shows a conceptual diagram of the simulated model developed in the present study. The life course, and the acquisition of frailty due to exposure to health insults is demonstrated through the gradient bars with blue representing lower frailty and red indicating higher frailty. The length of the gradient bars represents the survivorship of individuals while the color of the circles to the left of the gradient bars represents the frailty present from birth. The circles with arrows represent the experience of health insults, with the arrows representing the influence of an individual's frailty at time of exposure to the severity of the health insult, as well as the severity of the health insult due to the nature of the insult itself (represented by the size of the circle).

### 2.2 | Overview of the model

Following the generation of an initial cohort of 15 100 people, this model runs multiple iterations of a 120-year period in which members of this cohort accumulate stochastic frailty and eventually die. The frailty incurred differs based on the exposure to a health insult, the variable severity of the insult, and the multiplicative effect of individuals' pre-existing frailty value at time of exposure (Figure 1).

The model is highly theoretical and is designed to examine:

1. The individual variance in age-at-death occurring due to stochasticity in health insult exposure and stressor severity over five runs of the cohort

2. The degree to which birth frailty (the assigned frailty value at age 0) predicts age-at-death in this cohort, and therefore the contribution of stochasticity to determining age-at-death

The methodology used is an adaption of the approach taken by Hartemink et al. (2017) who used a gamma-Gompertz–Makeham model in which a gamma distributed frailty modifies the baseline Gompertz–Makeham mortality schedule. This study extends that previous work by generating health insults occurring in a probabilistic manner with variable severity (as opposed to a constant exposure with 5% frailty increase as in Hartemink et al. (2017)), through incorporating a measure of recovery in years without health insult exposure, and through the inclusion of the juvenile exponential decay component present in the Siler mortality model.

## 2.3 | Study cohort

The necessary population size (as determined by population mean age-at-death) to have comparable runs was examined through the comparison of the coefficient of variation (i.e., the ratio of a population's standard deviation to its mean also known as Epsilon or $E$) between runs. The amount of variation in the coefficient of variation yields the minimum population size necessary to overcome model stochasticity and produce replicable results at the population level (Lee et al., 2015; Lorscheid et al., 2012). The population size necessary to receive a stable coefficient of variation, commonly designated as a value of <0.01 variation between runs, was found to be 15 100 individuals (see Figure 2 for distribution of age-at-death and Table S1). The number of runs (5) was chosen to identify and demonstrate stability between runs.

Having established this necessary population size for stable outcomes at the population level between runs, a study cohort of 15 100 individuals aged 0 years are generated, with the initial frailty value (hereafter "birth frailty") and health insult exposure assigned using probabilistic distributions detailed below.

## 2.4 | Model design

### 2.4.1 | Mortality

The human age-predicted mortality risk is estimated in this model using the five-parameter competing hazard model described by Gage and Dyke (1986) based upon the mammalian mortality curve developed by Siler (1979). These demographic models of mortality in human populations demonstrate a "bathtub" or U-shaped curve in which the mortality rate is high in infancy (the immature component) before decreasing exponentially and stabilizing through childhood (the residual component) and the adolescent years, before increasing again in adulthood and increasing exponentially starting in middle age (the senescent component).

This can be described mathematically as $h(t) = a_1 e^{-b_1 t} + a_2 + a_3 e^{b_3 t}$.

In which time (here age) is $t$, the hazard value is $a$, the rate of change in hazard value is $b$, and thus the immature component is described by $a_1 e^{-b_1 t}$, the residual component $a_2$, and the senescent component $a_3 e^{b_3 t}$. The age-predicted hazards are fitted to a lifespan of up to 120 years through multiplication of the parameters by 120 (the duration of a single run of the simulation). This fitting does not limit the lifespan to 120 years of age; however, the likelihood of mortality at 120 years is essentially 100% and therefore substantially decreases the likelihood of surviving past this age. This lifespan is chosen to reflect the approximate natural biological lifespan of humans noting that not every individual will survive to this age as a result of exposure to health insults. The parameters used in the model were derived from life tables from 1841 England and Wales, provided by the Human Mortality Database as presented in Mitchell (1994) in order to model human mortality prior to the advent and widespread availability of modern medicine.

Although Siler models as applied to existing age-at-death data assume homogenous frailty, the use in the present study does not. Rather, the Siler mortality rate by age in the present study acts as a baseline which is modified by the frailty of individuals (both their birth frailty which remains a constant hazard throughout their lifespan, and their acquired frailty which arises from health insult exposures, but which also may reduce where recovery occurs) at each age as described in the following section. This multidimensional approach to frailty is in line with observations by Gage (1989) that individuals are likely not frail in one dimension only, but rather frailty is an emergent phenomenon of multiple interacting traits.

In the present study, the Siler model acts similarly to the mixed-Makeham mortality model described by Wood et al. (2002) but while retaining the juvenile exponential decay component which allows for more accurate modeling of age-specific risk of mortality in very young individuals. As simulation methods allow for very large sample sizes, especially of these young individuals frequently absent from archeological contexts, as well as accurate age determination the Siler model of mortality in this instance provides a more realistic mortality rate (Gage & Dyke, 1986). Given the departure from usual

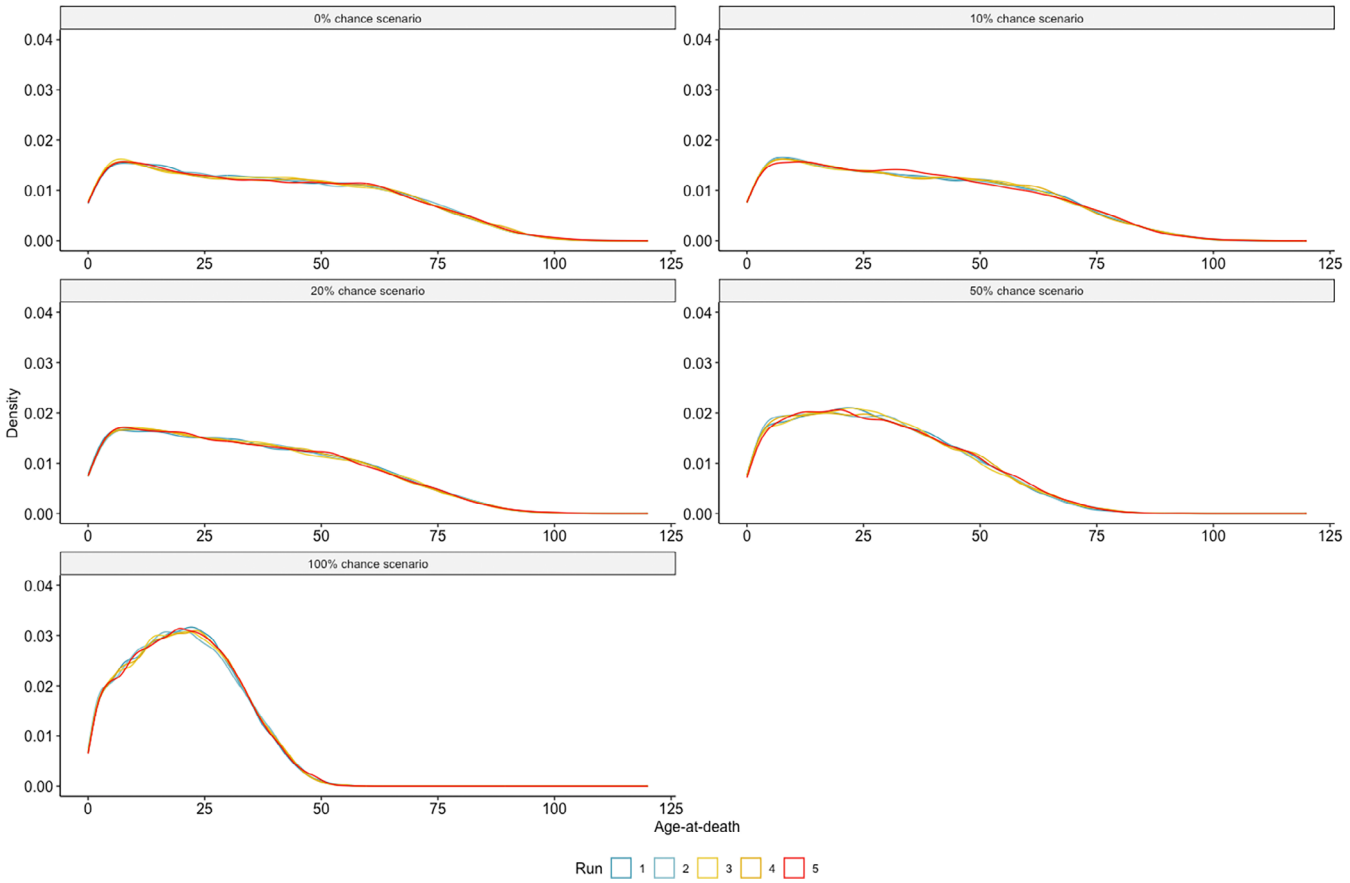


**FIGURE 2** Mean age-at-death across runs, per health insult exposure likelihood scenario. Figure 2 shows a density plot of age-at-death for each run of the simulation, stratified by health insult exposure likelihood scenario. This figure demonstrates that there is good consistency between each run of the model for all health insult exposure scenarios as indicated by the near identical overlap of each of the 5 colored lines which represent the five runs of the simulation.

paleodemographic approaches, comparison of age-specific mortality risk for the Siler model and the mixed-Makeham model are presented in the supporting information (Figures S1 and S2).

An individual's frailty at a given point in time, as described by Vaupel et al. (1979), is the degree of individual modification of the age-predicted force of mortality or the likelihood of mortality in relation to one's peers. For example, if an individual with a total frailty of one has an age-predicted likelihood of mortality of 0.05, they have a 5% chance of dying at this age. In comparison, an individual with a frailty accumulation of two will have twice the likelihood (10%), whereas an individual with an accumulation of 0.5 has half the likelihood (2.5%).

The likelihood of death in this model is therefore simulated by randomly drawing a number from 0 to 100 in each year of an agent's life; where this number is less than the calculated value of the age-predicted mortality hazard multiplied by the individual's total frailty, this individual dies. For instance, an individual with a frailty value of 1 and an age-specific mortality hazard of 2.5 will need to draw a number less than 2.5 in order to die in this year. An older adult with the same frailty will have an age-specific mortality risk that is much higher and thus the likelihood of drawing a number less than the age-specific mortality hazard is greater, reflecting the increasing likelihood of mortality with age.

### 2.4.2 | Frailty

*Birth frailty*

Birth frailty is a randomized value assigned to each individual when the cohort is generated. Frailty values are drawn from a gamma distribution, a distribution commonly used in the absence of a known distribution of frailty at birth (Weiss, 1990). The present study draws these birth frailty values from a gamma curve with a mean of 1 as produced by a shape of 10 and a scale of 0.1. These parameter values were chosen as they result in a distribution without excessively low or high values. The minimization of extreme outliers in the study cohort is

essential as the presence of excessively robust individuals (i.e., beyond the realm of biological possibility) may produce misleading results. This birth frailty value is designed to replicate the heterogeneous frailty from birth in a population arising from genetic, epigenetic, or congenital factors (Kuzawa & Quinn, 2009; McDade, 2005).

*Frailty arising from experiencing health insults ("acquired frailty")*

Beyond birth frailty, there are also the impacts of nonspecific health insults encountered by individuals over the course of their lives (hereafter "acquired frailty"). These may be infections, temporary nutritional insufficiency, chronic conditions, or any combination of these.

There are two necessary components to modeling acquired frailty, the likelihood of being exposed to a health insult each year, and the intrinsic severity of this insult if exposed. The total impact of exposure to an insult is then further moderated by the current frailty load of the individual. For each set of runs, the likelihood of exposure for each agent is determined sampling a number from 0 to 100 in each year, and where this number is less than the health insult threshold, exposure to a health insult occurs. The thresholds for the annual probability of a health insult varies across model scenarios: 0 (i.e., a 0% chance per year), 10 (i.e., a 10% chance per year), 20 (i.e., 20% chance per year), 50 (i.e., 50% chance per year), and 100 (guaranteed exposure every year).

In all scenarios, this exposure likelihood determines whether an individual will incur an increase in frailty via exposure to a health insult in the current year. Where exposed, a randomized frailty value (between 0.01 and 0.5) is then multiplied by the total frailty of the individual at this point in time. This adjusted frailty acquired frailty value is then added to a running total of acquired frailty experienced, thus far which informs the total frailty of this individual at this point in time. This approach is designed to reflect the amplified stress of stressor exposure based upon the existing frailty of an individual, and the accumulation of frailty over the lifespan.

*Resilience*

In years without exposure to a stressor, a small degree of recovery (5% reduction in the agent's acquired frailty total for each year of nonexposure) is included to simulate the dynamic nature of frailty throughout the lifespan. It is important to note that only the accumulated frailty from stressor exposure (acquired frailty) is reduced in instances of recovery years, whereas birth frailty remains unchanged, thus modeling the persistent influence of birth frailty.

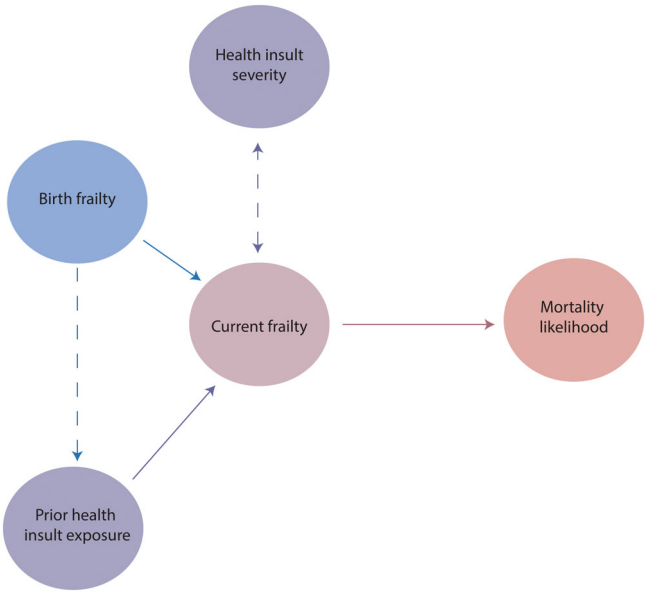


**FIGURE 3** Overview of frailty and mortality determination per year, per individual. Figure 3 shows a conceptual diagram of the contributing factors to frailty and mortality likelihood, per year of the simulation. In this diagram the current frailty of an individual (the center circle) is influenced by the frailty present from birth (the blue circle) and prior health insults (acquired frailty as represented by the lower left mauve circle), and in turn influences the severity of a health insult (the top circle), further contributing the degree of frailty and thus the likelihood of mortality at a given age (the red circle on the right).

*Total frailty*

The total frailty of an individual is the sum of the birth frailty and the acquired frailty accumulated at a given point in time. The total value therefore reflects the health status of an individual and informs the additional frailty incurred by subsequent health risk exposure, as well as the likelihood of mortality as detailed in the preceding section (Figure 3).

## 2.5 | Analysis methods

### 2.5.1 | Individual age-at-death variability

The variation in age-at-death per cohort size across five runs is evaluated through the comparison of the average range of age-at-death for individuals by set of runs.

### 2.5.2 | Predictive value of birth frailty

Having evaluated the individual variation in age-at-death arising from stochasticity, the predictive value of birth frailty on age-at-death is evaluated through linear

**TABLE 1** Variability in age-at-death across runs.

| Health insult exposure risk per year | Mean age-at-death | Mean range of age-at-death (years) | Mean minimum age-at-death | Mean maximum age-at-death |
|---|---|---|---|---|
| 0% | 37.7 | 52.5 | 12.4 | 64.9 |
| 10% | 36.1 | 50.4 | 11.9 | 62.3 |
| 20% | 34.1 | 47.7 | 11.4 | 59.1 |
| 50% | 28.2 | 37.9 | 10.2 | 48.1 |
| 100% | 20.5 | 24.5 | 8.4 | 32.9 |

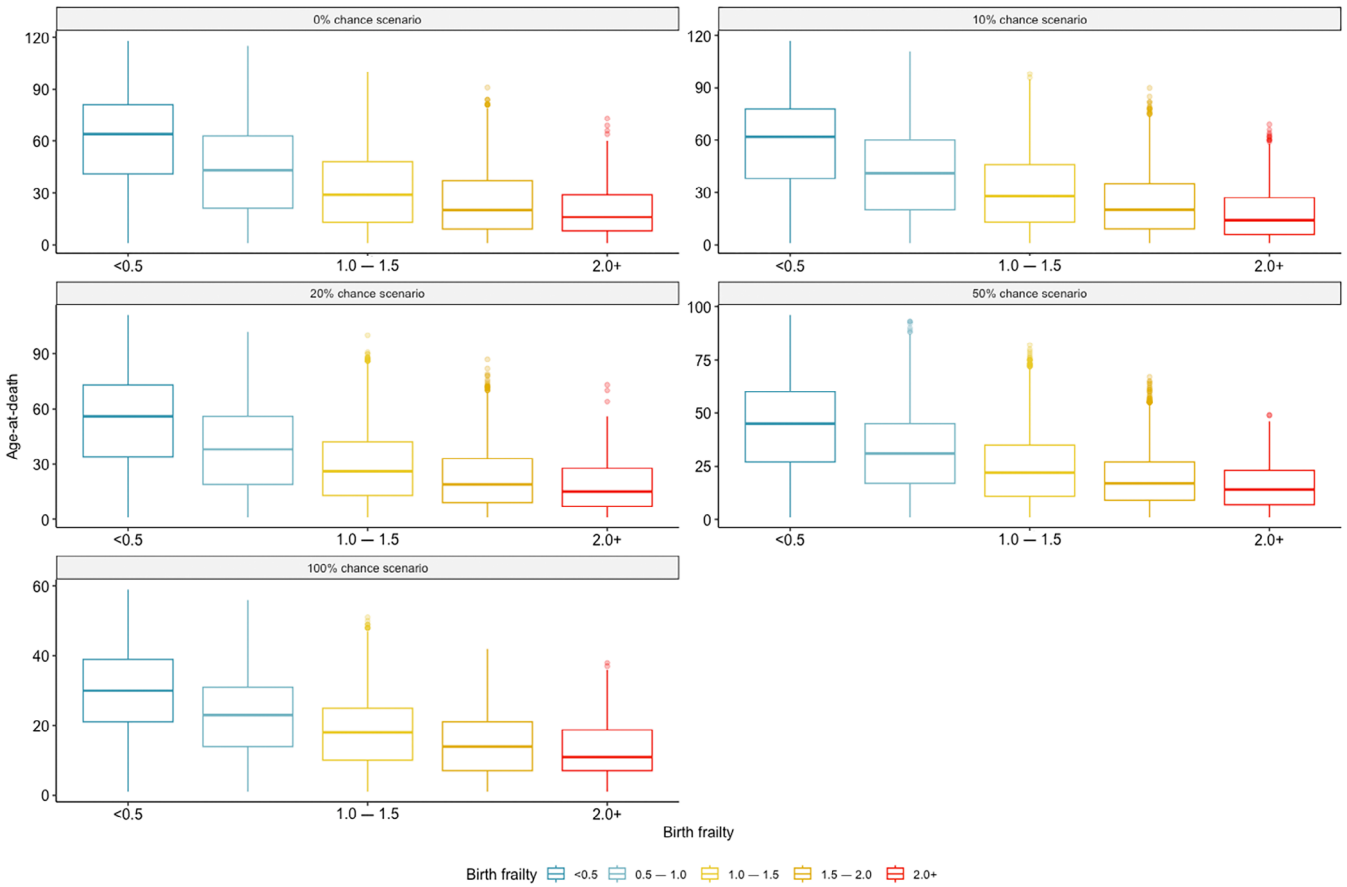


**FIGURE 4** Median age-at-death by birth frailty, by health insult exposure likelihood scenario. Figure 4 shows the median age-at-death and variance of age-at-death by the level of frailty present from birth across the pooled output of five runs of the simulation, stratified by health insult exposure likelihood scenario. A low birth frailty value means than an individual has a lower mortality risk compared to the reference age-at-death mortality risk while a high birth frailty value has a greater mortality risk than this reference risk. In this diagram the lowest birth frailties (dark blue) have the highest median age-at-death but also the widest range, with progressively younger median age-at-death and narrower range as birth frailty is increased. This is observed across all health insult exposure scenarios.

regression of age-at-death, by birth frailty from the pooled result of the five runs.

These models can be described mathematically as:

$$\widehat{\Upsilon} = \beta_0 + \beta_1\chi_1 + \beta_2\chi_2 \ldots + \beta_i\chi_i,$$

where $\widehat{\Upsilon}$ is the predicted value of the dependent variable (here mean age-at-death), $\beta_0$ is the intercept (i.e., the value of $\Upsilon$ when all independent variables are held at the reference level), $\chi_1$ through $\chi_i$ are the independent variables (here birth frailty), and $\beta_1$ through $\beta_i$ are the regression coefficients (i.e., the change in $\Upsilon$, with one unit change in the independent variable, holding all other variables constant).

The increase or decrease in age-at-death associated with birth frailties below or above 1.0–1.1 (the reference

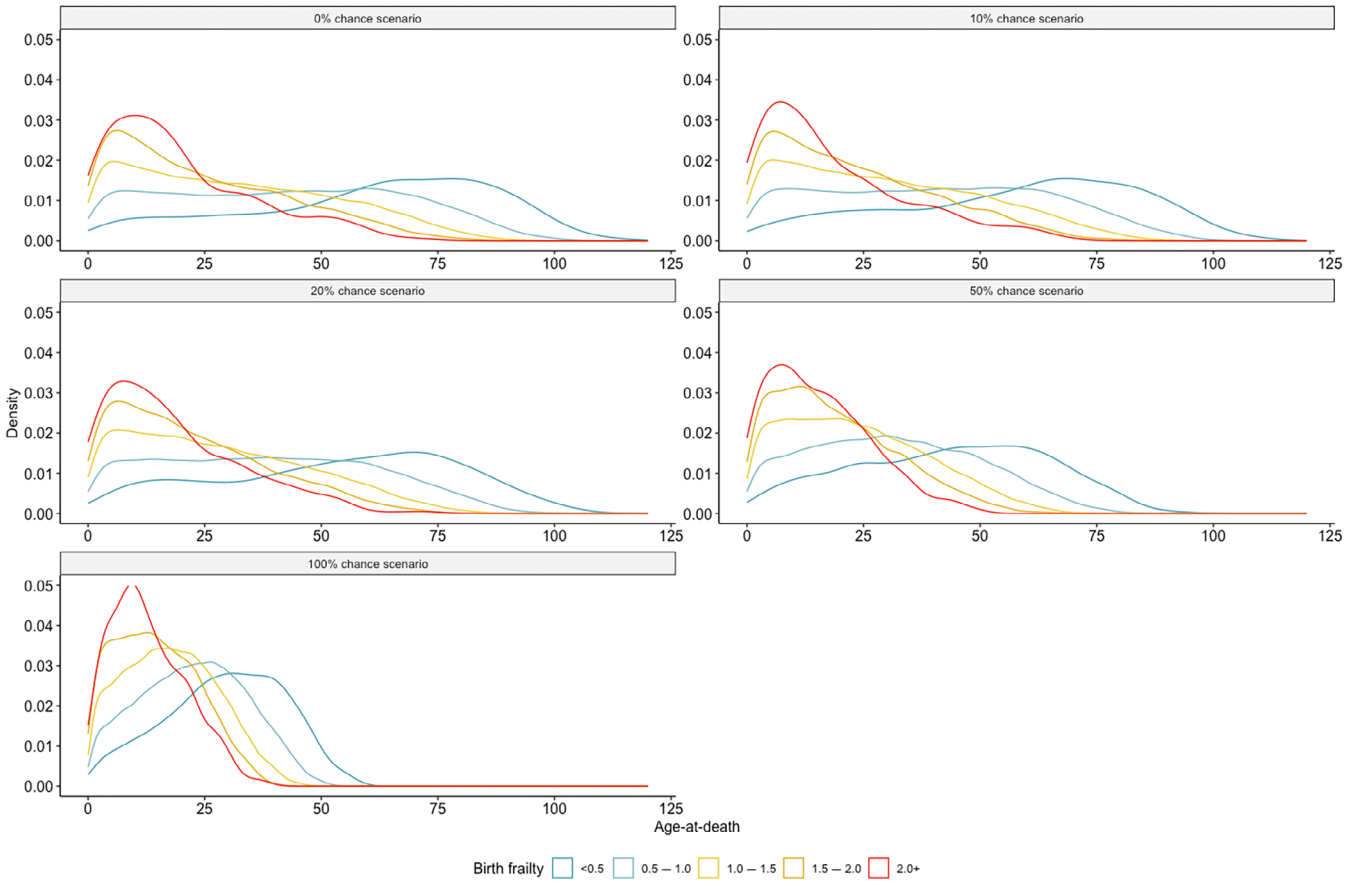


**FIGURE 5** Age at death distribution by birth frailty, by health insult exposure likelihood scenario. Figure 5 shows a density plot of the distribution of age-at-death by the level of frailty present from birth across the pooled output of five runs of the simulation, stratified by health insult exposure likelihood scenario. A low birth frailty value means than an individual has a lower mortality risk compared to the reference age-at-death mortality risk while a high birth frailty value has a greater mortality risk than this reference risk. For all health insult scenarios, the highest birth frailty (2.0+ in red) results in a greater proportion of deaths in younger ages, while the lowest birth frailty (<0.5, in dark blue) demonstrates greater survivorship into older ages. As health insult likelihood is increased, the peak of younger deaths becomes sharper, especially for the highest birth frailty category (in red) while the distribution of age-at-death for the least frail at birth cohort (dark blue) becomes compressed toward younger ages.

category) will be assessed for significance. The predictive value, that is, how well the birth frailty of an individual predicts age-at-death is determined from the adjusted $R^2$ value.

## 3 | RESULTS

### 3.1 | Individual age-at-death variability

Across the five runs, the mean age-at-death was oldest (37.7 years) for the scenario with no health insult exposure, and youngest (20.5 years) where exposure was guaranteed per year. The range of age-at-death for individuals was widest (i.e., highest variability) for the scenario with no exposure (52.5 years) and least in the guaranteed exposure scenario (24.5 years), with the highest mean minimum and maximum age-at-death also occurring in the 0% chance per year scenario (12.4 years and 4.9 years, respectively) and the lowest in the 100% chance scenario (8.4 and 32.9 years, respectively) (Table 1).

When accounting for birth frailty, the oldest mean age-at-death occurred in the lowest birth frailty category (<0.5), with a trend toward mean younger age-at-death with increasing birth frailty. The widest mean range of age-at-death occurred in the lowest birth frailty category (<0.5) for the 20%, 50%, and 100% scenarios. The widest mean range-of-death for the 0% and 10% scenarios was 0.5–0.6 birth frailty category. There was a uniform trend toward a narrower mean range of age-at-death and younger mean minimum and maximum age-at-death by increasing birth frailty (Table S2; Figures 4 and 5).

**TABLE 2** Multivariable linear regression.

| | Estimate | Standard error | *p* |
|---|---|---|---|
| Intercept | 35.3 | 0.110 | <.001 |
| <0.5 | 19.8 | 0.200 | <.001 |
| 0.5–0.6 | 13.5 | 0.160 | <.001 |
| 0.6–0.7 | 11.0 | 0.140 | <.001 |
| 0.7–0.8 | 7.9 | 0.130 | <.001 |
| 0.8–0.9 | 4.2 | 0.130 | <.001 |
| 0.9–1.0 | 1.5 | 0.130 | <.001 |
| 1.1–1.2 | −1.5 | 0.140 | <.001 |
| 1.2–1.3 | −3.0 | 0.140 | <.001 |
| 1.3–1.4 | −5.1 | 0.160 | <.001 |
| 1.4–1.5 | −6.1 | 0.180 | <.001 |
| 1.5–1.6 | −6.8 | 0.220 | <.001 |
| 1.6–1.7 | −7.9 | 0.260 | <.001 |
| 1.7–1.8 | −9.0 | 0.300 | <.001 |
| 1.8–1.9 | −10.1 | 0.420 | <.001 |
| 1.9–2.0 | −10.5 | 0.490 | <.001 |
| 2.0+ | −11.8 | 0.420 | <.001 |
| 10% chance scenario | −1.6 | 0.100 | <.001 |
| 20% chance scenario | −3.6 | 0.100 | <.001 |
| 50% chance scenario | −9.5 | 0.100 | <.001 |
| 100% chance scenario | −17.2 | 0.100 | <.001 |
| $R^2$ | Adjusted $R^2$ | | *p* |
| 0.187 | 0.187 | | <.001 |

### 3.2 | Predictive value of birth frailty

The predictive value of birth frailty on age-at-death was examined using a linear regression model on the pooled output of the five runs. In comparison to the reference birth frailty (1.0–1.1), lower birth frailty was associated with older age-at-death while higher birth frailty was associated with younger age-at-death. The lowest birth frailty was associated with a 20-year increase in age-at-death ($p < .001$), whereas the highest birth frailty was associated with a 12-year decrease in age-at-death ($p < .001$) (Table 2, Figure 6).

In comparison to the scenario with no health insult exposure, increased likelihood of exposure significantly decreased age-at-death with the greatest decrease observed for the guaranteed exposure scenario (a decrease of 17.0 years) (Table 2; Figure 7).

Despite these significant associations between birth frailty on age-at-death, however, the model had relatively low predictive value with birth frailty explaining 18.7% of the variance observed (Table 2). Examination of individual scenarios found that birth frailty alone explained between 10.2% and 12.1% of the variance observed for all scenarios (Figure 8; Table S3–S7).

Additional examination of age-at-death data generated through use of the mixed-Makeham mortality model finds that birth frailty has a greater influence on age-at-death than the Siler model with the combined birth frailty and health insult exposure likelihood scenario model explaining 35% of the variance observed. (Table S8).

## 4 | DISCUSSION

The findings of the present study demonstrate that the frailty of an individual at birth has relatively low predictive value (18.7%) on their age-at-death when also accounting for exposure likelihood. The predictive value per scenario (10.2%–12.1%) is similar to that of Hartemink et al. (2017) despite the inclusion of stochastic elements such as variable severity and recovery. Where mortality was generated using a mixed-Makeham model of mortality the predictive value of the full model was greater (35%) due to the use of birth frailty as the constant hazard component of this mortality model; however this still only accounts for a little over a third of the total variability observed. These findings suggest that, applied to a real population, the greatest contributions to mortality likelihood likely derive from factors that increase the likelihood of exposure to stressors, and to a larger extent the nature and timing of the stressors themselves, rather than "hidden heterogeneity" as traditionally conceptualized in bioarcheological research (i.e., heterogeneity arising from intrinsic factors such as phenotypes or prenatal environment). This is supportive of the findings by Tuljapurkar et al. (2009) in the context of reproductive success and survivorship in which stochasticity directly affects these measures of fitness, whereas heterogeneity from birth has far less influence on these outcomes, as well discussion by Gage (1989) regarding the likely multidimensionality of frailty and thus the low contribution of an individual aspect of frailty (here birth frailty) on age-at-death.

To be clear, intrinsic factors (as modeled by the birth frailty attribute in the simulation) play a vital role in survivorship, and in a real population would be moderated across generations and individual lifespans by extrinsic factors, but these intrinsic factors alone are not sufficient to reliably predict age-at-death as observed in this simulation. Thus, the role of stochasticity ("luck") in exposure to, and severity of, health insults is likely underappreciated in bioarcheological research and has implications for the interpretation and conceptualization of frailty when using age-at-death as a measure. We may understand the findings of the present study as reflecting the

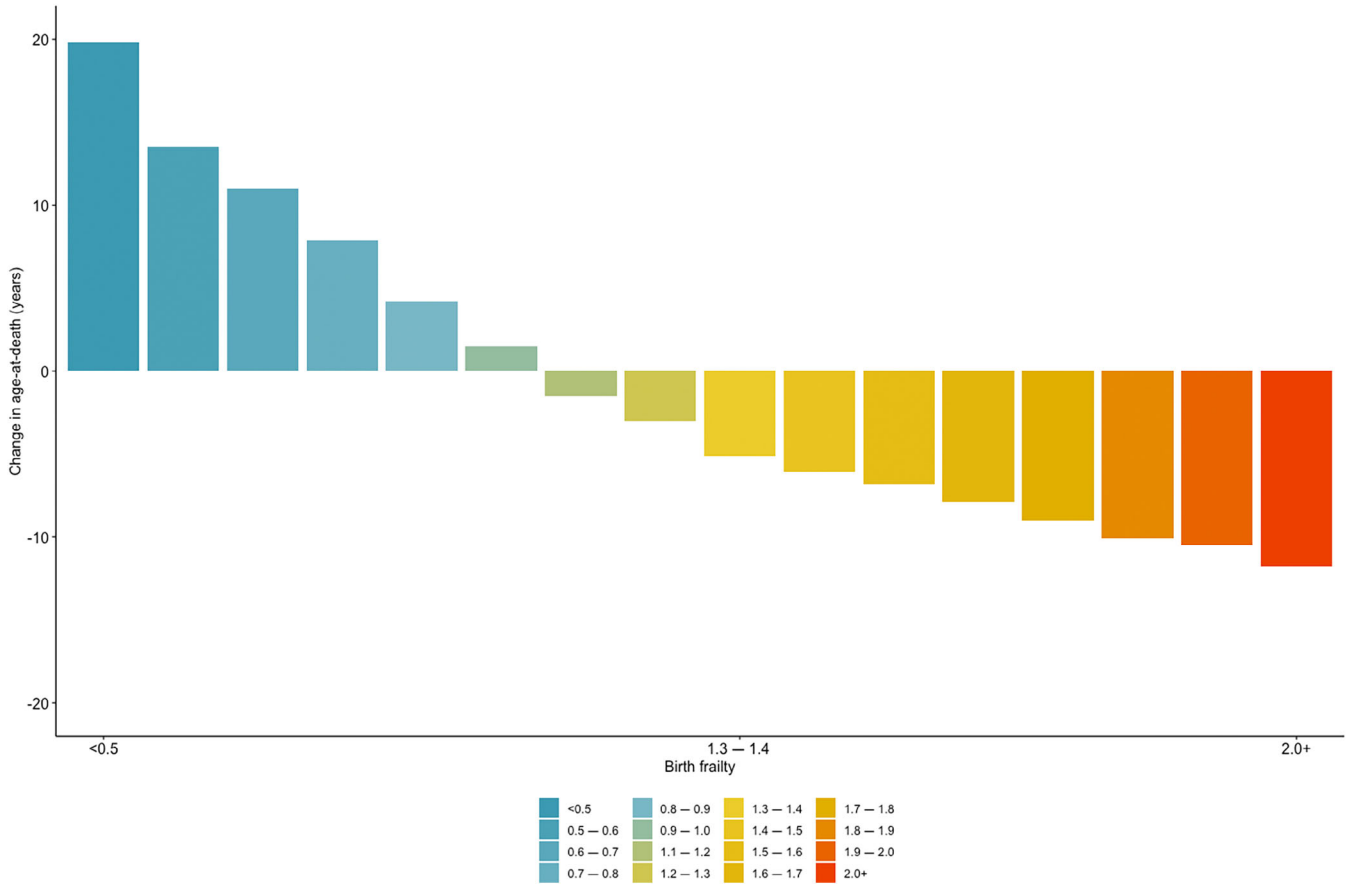


**FIGURE 6** Change in age-at-death associated with birth frailty. Figure 6 shows the difference in age-at-death by birth frailty in comparison to a birth frailty value of 1.0–1.1 as determined by the linear regression model. A low birth frailty value means than an individual has a lower mortality risk compared to the reference age-at-death mortality risk while a high birth frailty value has a greater mortality risk than this reference risk. Low birth frailty (in blues) have increased survivorship over the reference group with just under 20 years of additional survivorship noted for the <0.5 birth frailty cohort. Higher birth frailty (in yellows through to reds), conversely, decreased survivorship with a decrease in survivorship of just under 12 years noted for the 2.0+ birth frailty cohort.

greater potential lifespan for individuals of lower birth frailty, however the exposure (or not) to health insults and the impacts driven by this exposure ultimately determines an individual's age-at-death. Further, at given points in the lifespan such as early infancy or older age the "threshold" to mortality is much lower than at other ages, and thus it is not only the amount of frailty accumulated that is important but when this exposure occurs. It is important to note here also that the mortality likelihood, as determined by the five-parameter competing hazard model derived from the life-table data used in the present study, largely determines the population-level mean age-at-death. The variability in individual age-at-death is therefore additionally constrained by this "all cause" mortality risk.

In addition, the per-year exposure likelihood also influenced the individual variation in age-at-death, with lower likelihood scenarios having wider mean range of age-at-death than higher likelihood scenarios. This results in the situation where an individual with high birth frailty in the lowest likelihood scenario will have similar variability in age-at-death as a low birth frailty individual in a high likelihood scenario. This similarity in range reflects the combined influence of individual frailty and the circumstances they live in. Thus, exploration of age-at-death as a measure of frailty must consider (where possible) the broader landscape of risks in which individuals lived, that is, the nature and frequency of health insults.

These outcomes of these models—the pronounced variability of individual age-at-death across iterative runs of the same scenario; the limited predictive value of birth frailty; and the influence of health insult exposure likelihood and severity on age-at-death—may help to explain the mixed bioarchaeological evidence for any association between observable pathology in skeletal remains and age-at-death. For instance, linear enamel hypoplasia (LEH) has been associated with decreased survivorship

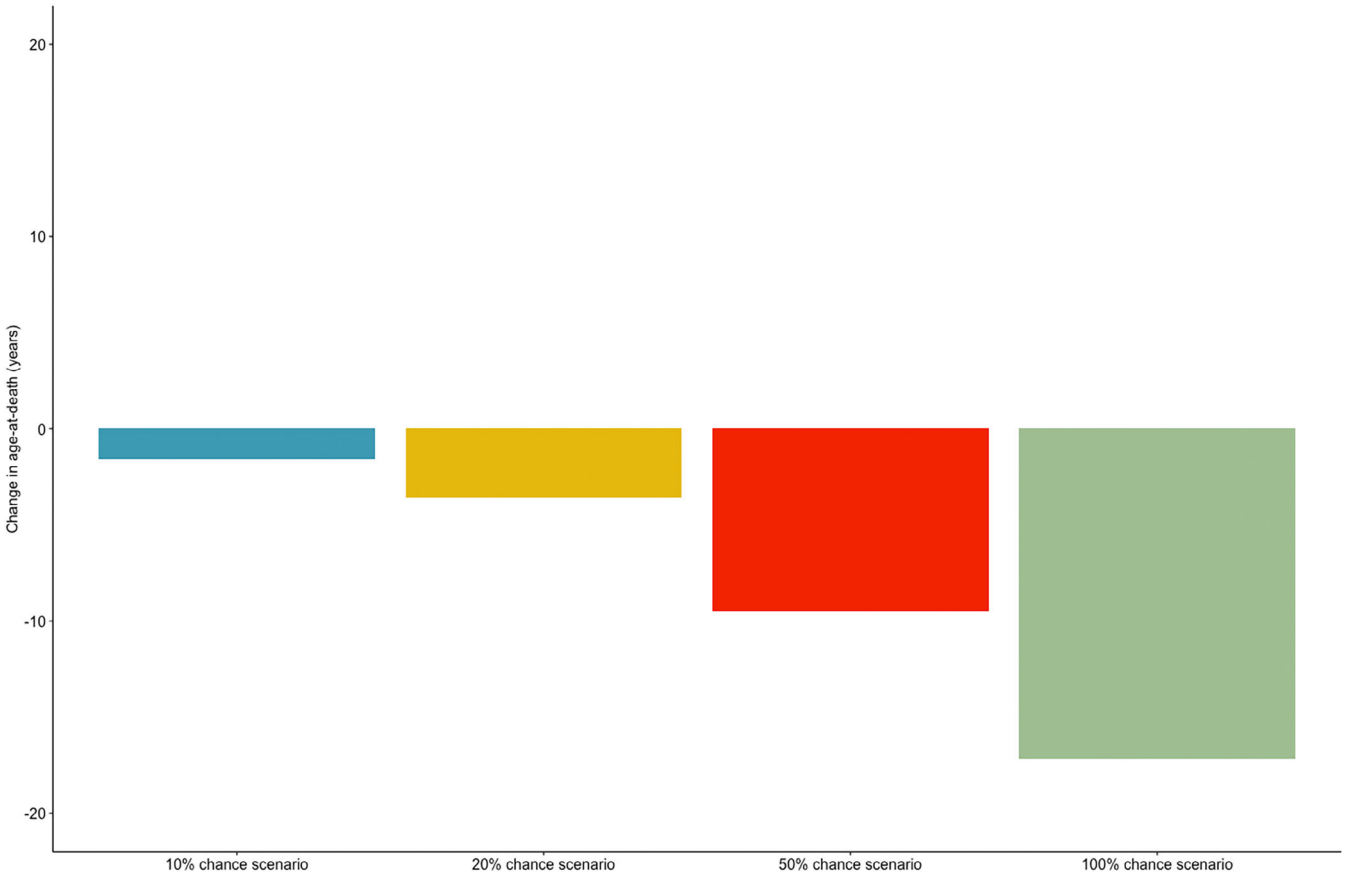


**FIGURE 7** Change in age-at-death associated with health insult exposure likelihood scenario. Figure 7 shows the difference in age-at-death by health insult exposure scenario in comparison to the scenario with no health insult exposure as determined by the linear regression model. Increasing the likelihood of health insult exposure decreases survivorship with the 10% chance per year scenario (in blue) decreasing survivorship by 1.6 years while the guaranteed exposure scenario (in red) decreased survivorship by just over 17 years in comparison the reference scenario (No exposure).

(see Boldsen (2007), and Ham et al. (2021)); however, Amoroso et al. (2014) find this association disappears when controlling for socio-economic status. They suggest that it is socioeconomic status; which largely drives exposure to both LEH-causing sources of stress and to subsequent health insults which ultimately reduce the lifespan of these individuals. The use of age-at-death as a measurement of frailty is subject to the influence of stochasticity in health insult exposure, and controlling for factors, which likely alter exposure likelihood may help to minimize the variance in age-at-death due to this stochasticity.

The high variability of individual age-at-death associated with stochasticity also has implications for the use of population sample subsets, especially where these subsets are very small (e.g. less than 100 individuals). Small sample size is a perennial issue in bioarcheology, though the emphasis has been largely on the likelihood of missing small effects (Milner & Boldsen, 2017) or of misleading results due to the influence of age structure (Klaus, 2014) rather than the likelihood of misleading trends arising due to stochasticity. Given the substantial variation in age-at-death between runs for individuals for each exposure scenario (ranges of 24.5 up to 52.5 years) in the present study, which is driven solely by stochasticity in exposure and severity of health insults, caution is advised in the interpretation of associations observed between visible skeletal pathology and age-at-death as skeletal indicators likely represent the "tip of the iceberg" in terms of health insults faced by individuals of past populations. The findings of the present study echo that of Kozak and Diachenko (2023) in their exploration of inter-site variation in skeletal indicators of scurvy and rickets presence, with risk of misinterpretation of pathology presence in small sample sizes noted by the researchers. Further work is needed to understand what sample size may be needed to accurately reflect the past population from which skeletonized remains derive; however, it is likely that this ideal minimum sample size will differ based upon the context of the population

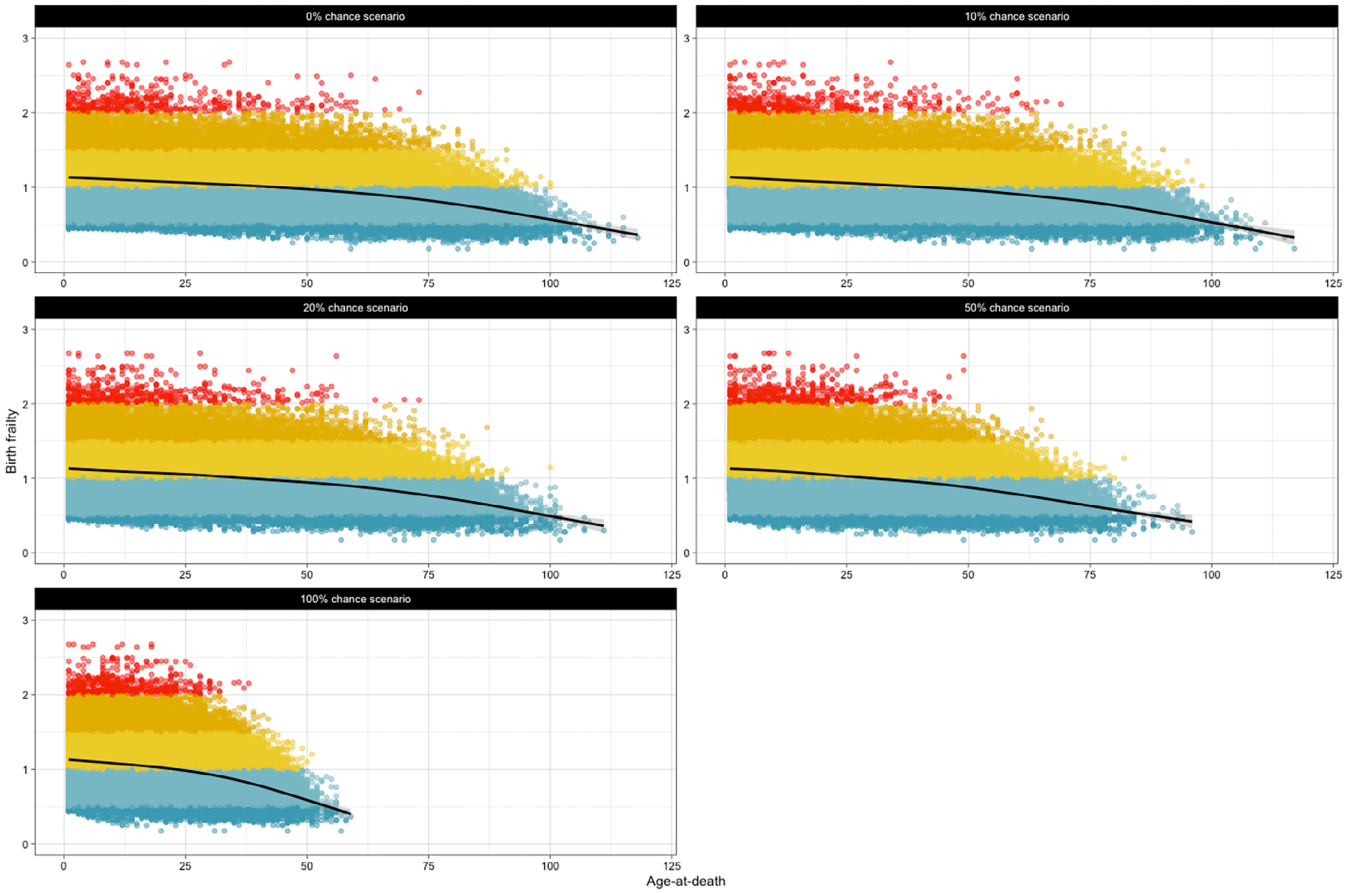


**FIGURE 8** Age-at-death by starting frailty for pooled runs, by health insult exposure likelihood scenario. Figure 8 shows the distribution of age-at-death by birth frailty per exposure likelihood with smoothed regression line (generated using a generalized additive model) to show trend. This figure shows increased variation in age-at-death for low birth frailty (in dark blue) and less variation for high birth frailty (in red). The distribution of age-at-death is additionally influenced by the health insult exposure likelihood scenario with wider distribution of age-at-death for all birth frailty cohorts in scenarios with no or low exposure risk per year, and compressed distribution of age-at-death when health insult exposure is higher or guaranteed per year.

(i.e., the nature and frequency of health insults, and factors which may influence these).

## 5 | CONCLUSION

This study demonstrates the influence of stochasticity in age-at-death (a measurement of frailty), at the individual level through simulation modeling. The findings of this simulation reinforce the need for caution when interpreting age-at-death as a proxy for frailty, especially in small samples. Further, the present study demonstrates the utility of simulation-based modeling in exploring aspects of frailty and mortality that are not observable from skeletal materials, thus providing complementary methods for better understanding of the past.

In parting, it is important to emphasize that a model is only as good as its parameters, and there remains much to discover about the dynamics underlying human longevity and frailty. The use of simulated population modeling in bioarcheology is not, therefore, pitched to replace the study of human skeletal remains but rather to help bridge the gap between research and broader theory building within the field. Further research using simulation to model factors associated with exposure likelihood, as well as factors which influence the intrinsic severity of a stressor (such as stressor type and developmental windows), will improve the theoretical understanding of frailty as explored in bioarchaeology. The outputs from increasingly sophisticated modeling, which draws upon the findings and methodology across scientific disciplines can then be incorporated into interpretative frameworks for bioarchaeologists working with skeletal remains.

## AUTHOR CONTRIBUTIONS

*Conceptualisation*: Bronwyn Wyatt. *Methodology*: Bronwyn Wyatt and Amy Anderson. *Formal analysis and*

*investigation*: Bronwyn Wyatt. *Writing–original draft preparation*: Bronwyn Wyatt. *Writing–review and editing*: Bronwyn Wyatt, Amy Anderson, Stacey Ward, and Laura A. B. Wilson. *Supervision*: Stacey Ward and Laura A. B. Wilson.

## ACKNOWLEDGMENTS

The authors would like to thank Dr. Clare McFadden for suggesting the use of simulation as a possible avenue to explore aspects of the osteological paradox and mortality trends of the past, and for organizing the Agent Based Modeling—Osteological Paradox Workshop in May 2023 which facilitated the discussions and collaboration that made this article possible. Open access publishing facilitated by Australian National University, as part of the Wiley - Australian National University agreement via the Council of Australian University Librarians.

## FUNDING INFORMATION

BW was supported by the Australian National University Research Scholarship (738/2018) and an Australian Government Research Training Program Scholarship, LABW was supported by the Australian Research Council (FT200100822).

## CONFLICT OF INTEREST STATEMENT

The authors have no relevant financial or nonfinancial interests to disclose.

## DATA AVAILABILITY STATEMENT

Code used to generate the study cohort, the simulation, and analysis are provided as supplementary materials, as well as the generated cohort and model output detailed in the present study.

## ORCID

*Bronwyn Wyatt* https://orcid.org/0000-0001-7259-0677
*Amy Anderson* https://orcid.org/0000-0002-9204-9076
*Stacey Ward* https://orcid.org/0000-0003-1725-0172
*Laura A. B. Wilson* https://orcid.org/0000-0002-3779-8277

## REFERENCES

Amoroso, A., Garcia, S. J., & Cardoso, H. F. V. (2014). Age at death and linear enamel hypoplasias: Testing the effects of childhood stress and adult socioeconomic circumstances in premature mortality. *American Journal of Human Biology*, *26*, 461–468.

Aphalo, P. (2023). ggpmisc: Miscellaneous Extensions to 'ggplot2'. R package version 0.5.5 ed.

Axtell, R. L., Epstein, J. M., Dean, J. S., Gumerman, G. J., Swedlund, A. C., Harburger, J., Chakravarty, S., Hammond, R., Parker, J., & Parker, M. (2002). Population growth and collapse in a multiagent model of the Kayenta Anasazi in long House Valley. *Proceedings of the National Academy of Sciences*, *99*, 7275–7279.

Bijwaard, G. E. (2014). Multistate event history analysis with frailty. *Demographic Research*, *30*, 1591–1620.

Boldsen, J. L. (2007). Early childhood stress and adult age mortality—A study of dental enamel hypoplasia in the medieval Danish village of Tirup. *American Journal of Physical Anthropology*, *132*, 59–66.

Carpenter, C., & Sattenspiel, L. (2009). The design and use of an agent-based model to simulate the 1918 influenza epidemic at Norway house, Manitoba. *American Journal of Human Biology*, *21*, 290–300.

Caswell, H. (2009). Stage, age and individual stochasticity in demography. *Oikos*, *118*, 1763–1782.

Caswell, H. (2014). A matrix approach to the statistics of longevity in heterogeneous frailty models. *Demographic Research*, *31*, 553–592.

Dewitte, S. N., & Hughes-Morey, G. (2012). Stature and frailty during the black death: The effect of stature on risks of epidemic mortality in London, A.D. 1348–1350. *Journal of Archaeological Science*, *39*, 1412–1419.

Dewitte, S. N., & Wood, J. W. (2008). Selectivity of black death mortality with respect to preexisting health. *Proceedings of the National Academy of Sciences*, *105*, 1436–1441.

Gage, T. B. (1989). Bio-mathematical approaches to the study of human variation in mortality. *American Journal of Physical Anthropology*, *32*, 185–214.

Gage, T. B., & Dyke, B. (1986). Parameterizing abridged mortality tables: The Siler three-component hazard model. *Human Biology*, *58*, 275–291.

Galeta, P., & Pankowská, A. (2023). A new method for estimating growth and fertility rates using age-at-death ratios in small skeletal samples: The effect of mortality and stochastic variation. *PLoS One*, *18*, e0286580.

Ham, A. C., Temple, D. H., Klaus, H. D., & Hunt, D. R. (2021). Evaluating life history trade-offs through the presence of linear enamel hypoplasia at Pueblo Bonito and Hawikku: A biocultural study of early life stress and survival in the ancestral Pueblo southwest. *American Journal of Human Biology*, *33*, e23506.

Hartemink, N., Missov, T. I., & Caswell, H. (2017). Stochasticity, heterogeneity, and variance in longevity in human populations. *Theoretical Population Biology*, *114*, 107–116.

Human Mortality Database As Presented In Mitchell, B. R. (1994). England and Wales total population life table for 1841, by sex and age from table 3: Population and vital statistics. In B. R. Mitchell (Ed.), *British historical statistics* (pp. 13–14). Cambridge University Press. www.mortality.org

Klaus, H. D. (2014). Frontiers in the bioarchaeology of stress and disease: Cross-disciplinary perspectives from pathophysiology, human biology, and epidemiology. *American Journal of Physical Anthropology*, *155*, 294–308.

Kozak, O., & Diachenko, A. (2023). Deficiency diseases in the Kyiv Rus' subadult population: The issue of the small sample effects. *Anthropologischer Anzeiger*, *80*, 363–383.

Kuzawa, C. W., & Quinn, E. A. (2009). Developmental origins of adult function and health: Evolutionary hypotheses. *Annual Review of Anthropology*, *38*, 131–147.

Lee, J.-S., Filatova, T., Ligmann-Zielinska, A., Hassani-Mahmooei, B., Stonedahl, F., Lorscheid, I., Voinov, A., Polhill, G., Sun, Z., & Parker, D. C. (2015). The complexities of agent-based modeling output analysis. *Journal of Artificial Societies and Social Simulation*, *18*, 4.

Lorscheid, I., Heine, B.-O., & Meyer, M. (2012). Opening the 'black box' of simulations: Increased transparency and effective communication through the systematic design of experiments. *Computational and Mathematical Organization Theory*, *18*, 22–62.

Marklein, K. E., Leahy, R. E., & Crews, D. E. (2016). In sickness and in death: Assessing frailty in human skeletal remains. *American Journal of Physical Anthropology*, *161*, 208–225.

Mcdade, T. W. (2005). Life history, maintenance, and the early origins of immune function. *American Journal of Human Biology*, *17*, 81–94.

Milner, G. R., & Boldsen, J. L. (2017). Life not death: Epidemiology from skeletons. *International Journal of Paleopathology*, *17*, 26–39.

O'Neil, C. A., & Sattenspiel, L. (2010). Agent-based modeling of the spread of the 1918–1919 flu in three Canadian fur trading communities. *American Journal of Human Biology*, *22*, 757–767.

R Core Team. (2021). *R: A language and environment for statistical computing* (4.1.2 ed.). R Foundation for Statistical Computing.

Ram, K., & Wickham, H. (2018). Wesanderson: A Wes Anderson Palette Generator. R package version 0.3.6 ed.

Reitsema, L. J., & Mcilvaine, B. K. (2014). Reconciling "stress" and "health" in physical anthropology: What can bioarchaeologists learn from the other subdisciplines? *American Journal of Physical Anthropology*, *155*, 181–185.

Robinson, D., Hayes, A., & Couch, S. (2023). Broom: Convert Statistical Objects into Tidy Tibbles. R package version 1.0.4 ed.

Romanowska, I., Wren, C. D., & Crabtree, S. A. (2021). *Agent-based modeling for archaeology: Simulating the complexity of societies*. SFI Press.

Siler, W. (1979). A competing-risk model for animal mortality. *Ecology*, *60*, 750–757.

Snyder, R. E., & Ellner, S. P. (2018). Pluck or luck: Does trait variation or chance drive variation in lifetime reproductive success? *The American Naturalist*, *191*, E90–E107.

Steckel, R. H., Sciulli, P. W., & Rose, J. C. (2002). A health index from skeletal remains. In *The Backbone of History: Health and Nutrition in the Western Hemisphere*, Steckel, R. H. & Rose, J. C. (eds.). Cambridge University Press. https://doi.org/10.1017/CBO9780511549953.004

Swedlund, A. C., Sattenspiel, L., Warren, A., Meindl, R. S., & Gumerman, G. J., III. (2016). Explorations in paleodemography: An overview of the artificial long House Valley agent-based modeling project. *New Directions in Biocultural Anthropology* In: Zuckerman, M. K. & Martin, D. L. (eds.). John Wiley & Sons, Inc. https://doi.org/10.1002/9781118962954.ch20.

Temple, D. H., & Goodman, A. H. (2014). Bioarcheology has a "health" problem: Conceptualizing "stress" and "health" in bioarcheological research. *American Journal of Physical Anthropology*, *155*, 186–191.

Tuljapurkar, S., Steiner, U. K., & Orzack, S. H. (2009). Dynamic heterogeneity in life histories. *Ecology Letters*, *12*, 93–106.

Usher, B. M. (2000). *A multistate model of health and mortality for paleodemography: Tirup cemetery*. The Pennsylvania State University.

Van Daalen, S., & Caswell, H. (2020). Variance as a life history outcome: Sensitivity analysis of the contributions of stochasticity and heterogeneity. *Ecological Modelling*, *417*, 108856.

Vaupel, J. W., Manton, K. G., & Stallard, E. (1979). The impact of heterogeneity in individual frailty on the dynamics of mortality. *Demography*, *16*, 439–454.

Weiss, K. M. (1990). The biodemography of variation in human frailty. *Demography*, *27*, 185–206.

Wickham, H. (2016). *ggplot2: Elegant graphics for data analysis*. Springer.

Wickham, H., Averick, M., Bryan, J., Chang, W., Mcgowan, L. D. A., François, R., Grolemund, G., Hayes, A., Henry, L., & Hester, J. (2019). Welcome to the Tidyverse. *Journal of Open Source Software*, *4*, 1686.

Wissler, A., & Dewitte, S. N. (2023). Frailty and survival in the 1918 influenza pandemic. *Proceedings of the National Academy of Sciences*, *120*, e2304545120.

Wood, J. W., Holman, D. J., O Connor, K. A., & Ferrell, R. J. (2002). Mortality models for paleodemography. In R. D. Hoppa & J. W. Vaupel (Eds.), *Paleodemography. Age distributions from skeletal samples*. Cambridge University Press.

Yaussy, S. L., Dewitte, S. N., & Hughes-Morey, G. (2023). Survivorship and the second epidemiological transition in industrial-era London. *American Journal of Biological Anthropology*, *181*, 646–652.

Yaussy, S. L., Dewitte, S. N., & Redfern, R. C. (2016). Frailty and famine: Patterns of mortality and physiological stress among victims of famine in medieval London. *American Journal of Physical Anthropology*, *160*, 272–283.

Zedda, N., Bramanti, B., Gualdi-Russo, E., Ceraico, E., & Rinaldo, N. (2021). The biological index of frailty: A new index for the assessment of frailty in human skeletal remains. *American Journal of Physical Anthropology*, *176*, 459–473.

Zhu, H. (2023). kableExtra: Construct Complex Table with 'kable' and Pipe Syntax.

## SUPPORTING INFORMATION

Additional supporting information can be found online in the Supporting Information section at the end of this article.

**How to cite this article:** Wyatt, B., Anderson, A., Ward, S., & Wilson, L. A. B. (2024). What's luck got to do with it? A generative model for examining the role of stochasticity in age-at-death, with implications for bioarchaeology. *American Journal of Human Biology*, e24115. https://doi.org/10.1002/ajhb.24115